Vol. 725: 29–44, 2023
https://doi.org/10.3354/meps14449

MARINE ECOLOGY PROGRESS SERIES
Mar Ecol Prog Ser

Published December 21

Oceanographic structuring of the mucous-mesh grazer community in the Humboldt Current off Peru

Dominik Auch[1,*], Vanessa Steinen[1], Luisa Steckhan[1], Rolf Koppelmann[1], Sadegh Yari[2], Volker Mohrholz[2], Anna Schukat[3], Mar Fernández-Méndez[4], Leila Richards Kittu[5], Myron A. Peck[6]

[1]Institute of Marine Ecosystem and Fisheries Science (IMF), University of Hamburg, 22767 Hamburg, Germany
[2]Leibniz Institute for Baltic Sea Research Warnemünde, 18119 Rostock, Germany
[3]Bremen Marine Ecology, University of Bremen, 28359 Bremen, Germany
[4]Alfred-Wegener-Institut, Helmholtz-Zentrum für Polar- und Meeresforschung, 27570 Bremerhaven, Germany
[5]GEOMAR Helmholtz Centre for Ocean Research Kiel, 24148 Kiel, Germany
[6]Department of Coastal Systems (COS), Royal Netherlands Institute for Sea Research (NIOZ), 1797 SZ 't Horntje, Texel, The Netherlands

ABSTRACT: The Humboldt Upwelling System (HUS) supports high levels of primary production and has the largest single-stock fishery worldwide. The high fish production is suggested to be related to high trophic transfer efficiency in the HUS. Mucous-mesh grazers (pelagic tunicates and gastropods) are mostly of low nutritious value and might reduce trophic transfer efficiency when they are locally abundant. Unfortunately, little is known about the spatial dynamics of mucous-mesh grazers from Peruvian waters, limiting our understanding of their potential ecological role(s). We provide a spatial assessment of mucous-mesh grazer abundance from the Peruvian shelf in austral summer 2018/2019 along 6 cross-shelf transects spanning from 8.5 to 16° S latitude. The community was dominated by appendicularians and doliolids. Salps occurred in high abundance but infrequently, and pelagic gastropods were mostly restricted to the north. At low latitudes, the abundance of mucous-mesh grazers was higher than some key species of crustacean mesozooplankton. Transects in this region had stronger Ekman transport, higher temperature, lower surface turbidity and a broader oxygenated upper water layer compared to higher-latitude transects. Small-scale lateral intrusions of upwelled water were potentially associated with high abundances of doliolids at specific stations. The high abundance and estimated ingestion rates of mucous-mesh grazers in the northern HUS suggest that a large flux of carbon from lower trophic levels is shunted to tunicates in recently upwelled water masses. The data provide important information on the ecology of mucous-mesh grazers and stress the relevance to increase research effort on investigating their functioning in upwelling systems.

KEY WORDS: Gelatinous zooplankton · Abundance · Humboldt Upwelling System

1. INTRODUCTION

Eastern Boundary Upwelling Systems (EBUSs), located at the eastern coastlines of the Atlantic and Pacific Oceans, are among the most productive marine ecosystems worldwide and support economically valuable commercial and culturally important artisanal fisheries (Pauly & Christensen 1995, Cole & McGlade 1998, Vargas et al. 2007). Driven by equatorward winds, surface water masses are pushed offshore and replaced by upwelled deep water providing strong nutrient supply to the euphotic zone. The

*Corresponding author: auch.dominik@web.de

Publisher: Inter-Research · www.int-res.com

4 major EBUSs (California Upwelling System, Humboldt Upwelling System [HUS], Canary Upwelling System and Benguela Upwelling System) have high annual rates of primary production. In the California Upwelling System, production rates (323 g C m^{-2} yr^{-1}) are similar or somewhat lower compared to the Benguela (517 g C m^{-2} yr^{-1}), Canary (539 g C m^{-2} yr^{-1}) and Humboldt (566 g C m^{-2} yr^{-1}) Upwelling Systems (Chavez & Messié 2009). Fishery catches, however, are about 6- to 10-fold higher in the HUS (36–89 mg C m^{-2} d^{-1}) compared to the other systems (6–8 mg C m^{-2} d^{-1}) (Chavez et al. 2008).

The Peruvian anchovy *Engraulis ringens* fishery in the HUS is the largest single-stock fishery worldwide, contributing about 10% of the annual global fishery yield (FAO 2021). The background for this increased fish production in the HUS compared to other EBUSs has been reviewed thoroughly (Chavez et al. 2008), and various hypotheses exist. For example, the outstanding fishery yield may be related to the close proximity of the HUS to the equator, resulting in stronger upwelling at low wind conditions and periodic re-setting of the food web (particularly predators of anchovy) due to El Niño–Southern Oscillation (Bakun & Weeks 2008), high ichthyoplankton retention rates during strong upwelling that favor anchovy recruitment (Brochier et al. 2011) or a high trophic transfer efficiency from primary producers to fish (Chavez et al. 2008). The latter might be related to a short trophic pathway or shoaling of the oxygen minimum zone which concentrates predators and prey in near-surface waters (Taylor et al. 2008, Schukat et al. 2021). These explanations are not mutually exclusive. Even though the hypothesis of primary producers as the main prey resource of adult small pelagic fish (Ryther 1969) has been rejected (Espinoza & Bertrand 2008), a short classical food chain is widely assumed to support high trophic transfer efficiency, and direct feeding on phytoplankton diet is of high importance for the larvae of some anchovy species (Scura & Jerde 1977). This 'classical' food web in the HUS is assumed to be dominated by large primary producers (mostly large diatoms), herbivorous mesozooplankton micronekton (such as calanoid copepod species or krill) and small pelagic fish (González et al. 2004).

The importance of mucous mesh-grazers, a group of tunicates and pelagic mollusks which are traditionally seen as 'trophic dead ends', could be expected to be low in a 'classical' food web with high trophic transfer efficiency (Conley et al. 2018). However, accumulating evidence indicates that the microbial food web might play a much more important role in coastal upwelling areas than traditionally considered (Neuer & Cowles 1994, Cuevas et al. 2004, Vargas et al. 2007, Rocke et al. 2020). While key crustaceans such as copepods and euphausiids effectively feed on 'larger' prey, with copepods having consumer:prey size ratios of ~10:1 to 30:1 for 50% relative clearance rates (Hansen et al. 1994), understudied mucous-mesh grazers (thaliaceans, thecosome pteropods) can effectively feed on much smaller particles, exceeding consumer:prey size ratios of 10 000:1 (Conley et al. 2018). In the case of appendicularians, particles as small as viruses can be consumed (Lawrence et al. 2018). Hence, the link between mucous-mesh grazers and the microbial food web may be a pathway through which mucous-mesh grazers play a much more important role in coastal upwelling areas than traditionally considered. These gelatinous taxa such as tunicates, which can have high individual and population growth rates under suitable environmental conditions (Deibel & Lowen 2012), may also play an important role in the export of carbon from pelagic to deeper waters (Luo et al. 2020) via the rapid sinking rates of large salp fecal pellets and export of organic matter in appendicularian houses and carcasses towards the seafloor (Perissinotto & Pakhomov 1998, Luo et al. 2020, 2022). However, despite their potentially high relevance to marine biogeochemical and trophodynamic processes (Henschke et al. 2016), the role of mucous-mesh grazers in the HUS is largely unexplored (Ayón et al. 2008).

Upwelling systems are physically dynamic systems in terms of changes in upwelling intensity and mixing processes (Rossi et al. 2009, Gruber et al. 2011), with pronounced variability observed both temporally (e.g. short upwelling pulses to long-term climatic effects) and spatially (e.g. small filaments to large oceanographic currents). The effects of variable environmental conditions on mucous-mesh grazer community dynamics within the HUS are largely unknown. Lavaniegos & Ohman (2003) classified pelagic tunicates of the California current into cool-phase and persistent groups. The occurrence of patches of mucous-mesh grazers is difficult to predict (Boero et al. 2008), and patches can be of various sizes ranging from a few kilometers to >100 km in width (Paffenhöfer & Lee 1987, Deibel & Paffenhöfer 2009). In the present study, we used a spatial sampling approach to investigate (1) whether the abundance and composition of the mucous-mesh grazer community was related to differences in regional hydrographic conditions with a special emphasis on upwelling intensity and (2) whether the spatial pattern of mucous-mesh grazers was related to primary

production and/or the abundance and species composition of copepods, in order to (3) provide insights into the potential trophodynamic role of mucous-mesh grazers in the HUS.

2. MATERIALS AND METHODS

2.1. Sampling

Sampling was carried out during cruise MSM80 of the RV 'Maria S. Merian' along the Peruvian coastline (8.5–16° S, Fig. 1). Samples were mainly collected at stations along inshore–offshore transects. Samples were taken both day and night (at time of arrival at the station) from 27 December 2018 at 8.5° S (Transect 1, T1) to 25 January 2019 at 16° S (T6). Transect locations were partly based on the knowledge of the anchovy spawning grounds covering the northern stock (T1 and T2) and the southern stock (T5 and T6). For taxonomic analyses of mucous-mesh grazers, 42 oblique hauls with a multiple closing net (MCN, 0.25 m^2 net opening, equipped with a flowmeter; MultiNet Midi, Hydro-Bios) were conducted at a vessel speed of 2 knots. A station/net overview is provided in Table S1 in the Supplement at www.int-res.com/articles/suppl/m725p029_supp.pdf. Three nets per haul with a mesh size of 300 µm were analyzed. In general, the upper 100 m interval (or the entire water column at stations with shallower depths) was sampled in 3 depth ranges: below, within and above the thermocline. Where the water column was largely well mixed and homogenized, similar depths were used as at nearby stations. Crustacean mesozooplankton were sampled with vertical MultiNet hauls (MCN, 0.25 m^2 net opening, mesh size 200 µm, MultiNet Midi, Hydro-Bios). All MultiNet samples were immediately preserved in a solution of 4% formaldehyde buffered with sodium-tetraborate in filtered seawater. At each station, a conductivity, temperature, depth (CTD) meter (Sea-Bird SBE 911plus) measured temperature, salinity, oxygen and turbidity. Water samples from CTD casts were taken for HPLC analyses providing chlorophyll *a* (chl *a*) concentrations (profiles provided in Fig. S1) and taxonomical data from 4–7 depths within the upper 100 m. Additionally, high-resolution temperature and salinity measurements were made using a ScanFish II undulating CTD (EIVA a/s) equipped with a Seabird 911+ CTD along sampling transects. ScanFish II sampling was conducted a maximum of 1 d before the start or 1 d after the completion of net sampling at the respective transect.

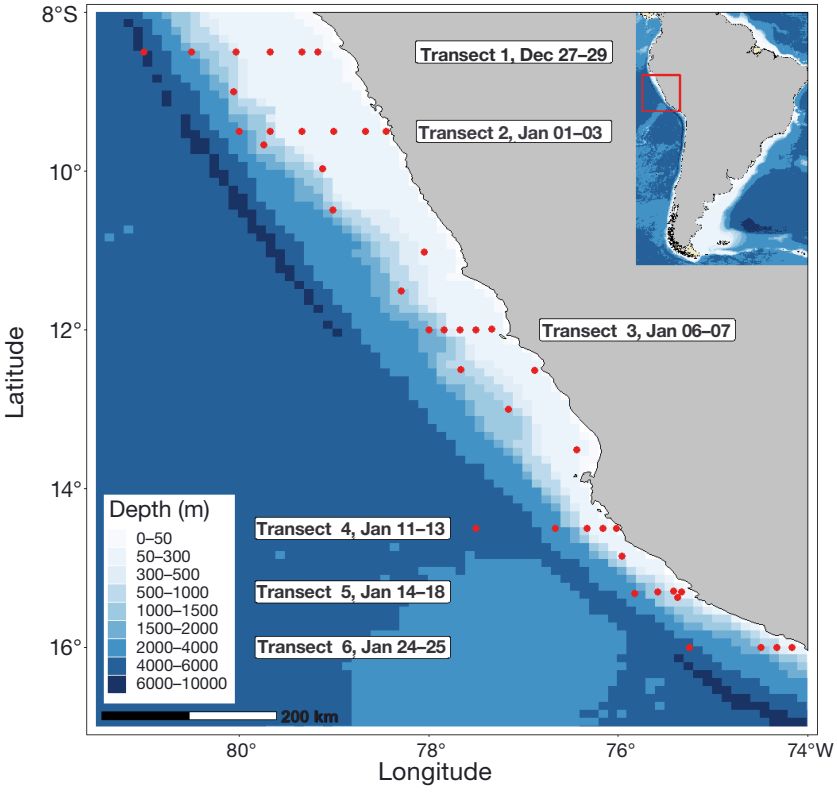

Fig. 1. Sampling locations (red dots) during cruise MSM80 of the RV 'Maria S. Merian', including the 6 transects. The red rectangle in the inset shows the study location along the western coast of South America

2.2. Laboratory work

In the laboratory, samples were transferred into sorting fluid consisting of 5% propylene glycol, 0.5% propylene phenoxytol and 94.5% tap water (Steedman 1976). If necessary, samples were subsampled using a Folsom plankton splitter, and all mucous-mesh grazers and copepods were identified to species level whenever possible using a stereo-microscope (Leica M165C and MZ12.5). For a substantial proportion of the mucous-mesh grazers, however, species identification was not possible due to the fragility of specimens. Appendicularians were only identified to family level. Thaliacean life stages were not separated, and buds were excluded from taxonomic analyses.

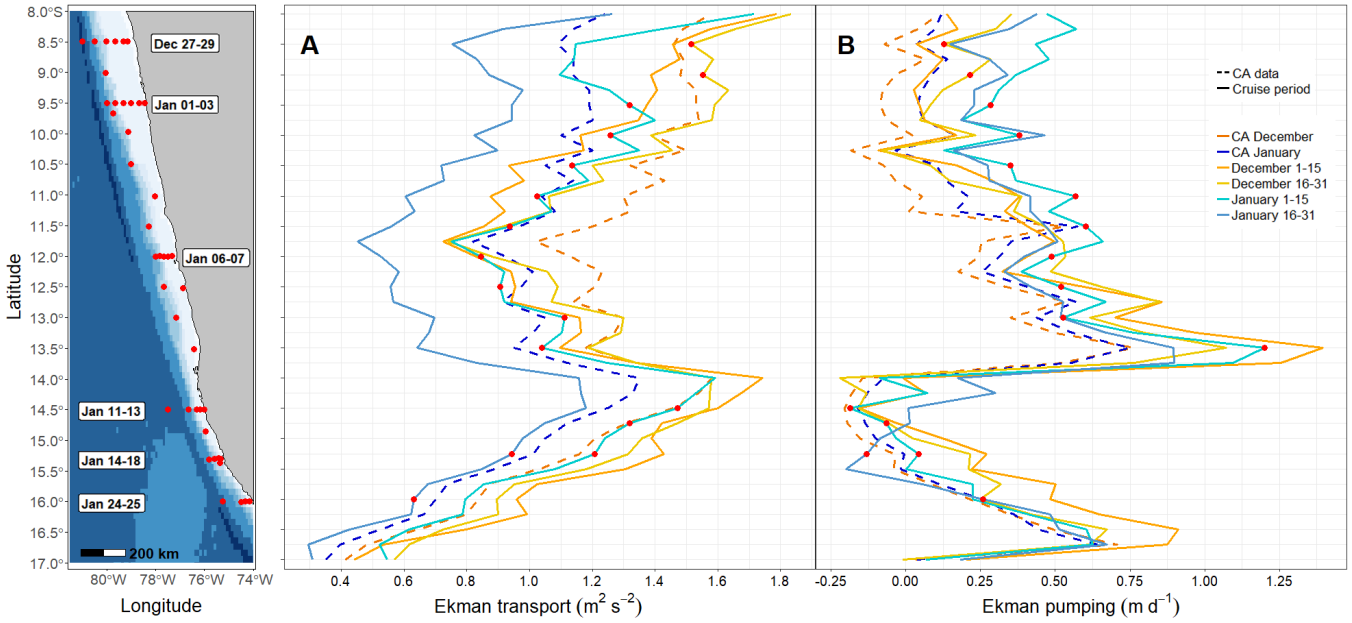

Fig. 2. Upwelling parameters calculated along the latitudinal gradient of the study region. (A) Ekman transport was calculated for a 100 km band from shore. (B) Ekman pumping was calculated for the 50–100 km band from shore. Dashed lines represent climatological averages (CAs) of the austral summer months January and February. Two-week averages are depicted with solid lines for December 2018 (orange colors) and January 2019 (blue colors). Red points on solid lines indicate the sampling periods at the respective latitudes

2.3. Data analysis

Chl *a* measurements were derived from HPLC analysis. Upwelling was characterized by curl-driven upward velocity, representing the more spatially widespread upwelling, and the Ekman transport as a unit of offshore transport and coastal upwelling (Fig. 2). Regarding Ekman transport (Fig. 2), originally negative numbers indicating westward transport of water masses were transformed to positive values to improve comparability with Ekman pumping and to make data more intuitive. Herein, descriptions of upwelling comprise the period of sampling and the 2 wk period before sampling, as upwelling signals might result in a delayed response in zooplankton. Ekman transport averages are provided for a grid (25 km resolution) within a range of 100 km from the coast. Due to characteristics of wind-stress curl, the Ekman pumping estimation is valid for areas 50–100 km to shore. Additionally, the climatological mean values (1980–2019) for Ekman transport and Ekman pumping for the months of December and January are provided. The upwelling data were based on the wind product of ERA5 data sets provided by the European Centre for Medium-Range Weather Forecasts. The comparison of ingestion rates of gelatinous groups and copepods was based on stocks, as the variable sampling depths between both data sets hampered a comparison of depth-specific abundance. Ingestion rates of stocks were calculated based on literature values per specimen

Table 1. Literature values used for ingestion rate (IR) calculations. The IR estimate for the most dominant mucous-mesh grazer species was used for the calculation of the IR of the entire family

Species group	Species	IR (µg C ind.$^{-1}$ d^{-1})	Reference
Copepoda	*Calanus chilensis*	3.6	Boyd et al. (1980)
	Centropages brachiatus	3.8	Vargas & González (2004)
	Nannocalanus minor	5.1	Schukat et al. (2013)
Oikopleuridae	*Oikopleura longicauda*	4.2	Vargas & González (2004)
Doliolidae	*Doliolum denticulatum*	21.0	Katechakis et al. (2004)
Salpidae	*Iasis cylindrica*	36.87	González et al. (2000)

(Table 1) multiplied by stocks. Since information on mucous-mesh grazer ingestion rates is scarce, values of the most abundant species were used as representative numbers for the respective families.

2.4. Statistical analysis

The station map (Fig. 1) was prepared using the R package 'ggOceanMaps' and the ETOPO1 1ARC-minute global relief model from NOAA (Amante & Eakins 2009). The zooplankton counts were standardized to ind. m^{-3}. Statistics and graphs were compiled at the family level in order to prevent biases related to individuals that could not be identified to species level. The vertical distribution was analyzed by calculating the weighted mean depth (WMD) following Pearre (1973): $WMD = \Sigma (n_i\ d_i) / \Sigma\ n_i$, where n is the abundance in ind. m^{-3} and d is the center of the sampled depth interval in meters. The comparison of vertical distributions of day and night was exclusively based on samples outside twilight periods. Subsequently, the significance of day–night differences and between north and south was assessed for the most abundant families ($n \geq 5$ per factor level) with Mann-Whitney tests. Nonmetric multidimensional scaling (NMDS) was conducted using R ('vegan' package, Oksanen et al. 2020) in order to get insight on potential differences in mucous-mesh grazer community composition and its drivers. The analyses were exclusively conducted for mucous-mesh grazer data and abiotic parameters from 3 depth bins (5–15, 16–30 and 31–50 m). As the oxygen concentration limits the occurrence of many dominant taxa within the HUS to lower depths, we restricted the analysis on potential drivers to the upper 50 m. Categories for latitude (north: Stations [Stns] 1–36, center: Stns 38–66, south: Stns 67–104) and topography (oceanic: >2000 m, slope: 200–2000 m, shelf: 100–200 m, coast: <100 m) were formed to account for difference in latitudinal and inshore–offshore distribution. Upwelling data were provided as one value per latitude per day. For the analysis, the first and second half of a month were averaged separately. Subsequently, the value from the period in which the sampling was conducted was considered 'while sampling' and the period before was denoted as 'before sampling'. For the NMDS, abundance data were square-root transformed to account for the high dominance of individual families within the gelatinous community and Bray-Curtis distance was used. Environmental parameters were fitted using the 'ENVFIT' function (Oksanen et al. 2020). Significance outcomes and further common testing results (ANOSIM and Mantel's test) are not presented for several reasons. First, Moran's *I*-tests indicated spatial autocorrelation for the majority of both independent and dependent variables. Furthermore, distinguishing between the effects of individual drivers was hampered by high levels of collinearity of environmental variables. In addition, the spatial resolution of potential drivers was not consistent. For upwelling parameters, only one value per latitude exists. Local effects might therefore be masked by high longitudinal variability. Chl *a* and crustacean data were entirely excluded from NMDS analyses in order to prevent loss of data points when exclusively using fully overlapping stations. Other potential drivers such as currents or water masses were also not included. Hence, a meaningful statistical comparison of all drivers was not possible.

3. RESULTS

3.1. Upwelling parameters

Ekman transport (Fig. 2A) was variable across latitudes during the cruise period, but broadly followed the climatological averages for December and January with 2 peaks observed (8–10° S and around 14° S) across the sampling area. In general, coastal upwelling was stronger in December than in January. At T1 (8.5° S, 27–29 December), strong upwelling (~1.5 $m^2\ s^{-1}$) was prevalent during the first and last 2 wk periods of December. At T2 (9.5° S, 1–3 January), Ekman transport was higher during the second half of December (~1.6 $m^2\ s^{-1}$) and the first half of January (~1.3 $m^2\ s^{-1}$) in comparison to the monthly climatological averages of the respective months. At 12° S (T3, 6–7 January), Ekman transport during the first half of January (~0.85 $m^2\ s^{-1}$) and the last 15 d of December (~0.85 $m^2\ s^{-1}$) was lower than long-term climatological averages for these time periods. Towards 14° S, Ekman transport reached its second peak value and was relatively high (~1.45 $m^2\ s^{-1}$ during the first 15 d of January) at T4 (14.5° S, 11–13 January) where coastal upwelling had also been strong in the second half of December (~1.55 $m^2\ s^{-1}$). Further south, Ekman transport rapidly declined to values partly below climatological averages at T5 (15.3° S, 14–18 January, ~1.2 $m^2\ s^{-1}$ for the first half of January and ~0.95 $m^2\ s^{-1}$ for the second half) and T6 (16° S, 24–25 January, ~0.8 $m^2\ s^{-1}$ for the first half of January and ~0.63 $m^2\ s^{-1}$ for the second half).

In contrast to Ekman transport, curl-driven upwelling (Ekman pumping) was relatively intense and highest in the central portion of the sampling area with local minima at 10.25° S and around 14.5° S (Fig. 2B). The Ekman pumping calculated for the cruise period was higher than the long-term climatological average, with a peak at 13.5° S, a local minimum at 14–15.5° S and a second peak at ~16.5° S (Fig. 2B). On the temporal scale, there was an increase in Ekman pumping from the beginning of December towards the end of January in the north, but an opposite trend was observed south of 12° S with an exception between 14 and 14.75° S (compare lines showing bi-weekly periods in Fig. 2B).

3.2. Additional hydrographical parameters

In general, the Peruvian shelf is broad and shallow in the north and narrows towards the southern waters off Peru. In the north, surface waters were largely dominated by warm subtropical surface water except for a coastal band of 100 km, where shelf waters were largely homogenized and, hence, subsurface waters were colder than further offshore (Fig. 3A,B). At distances >100 km, the vertical temperature profile of T1 was distinctly stratified. At T2, the vertical temperature gradient was narrower. Further south (Fig. 3C–F), the upper mixed water layer was closer to the surface compared to T1 and T2. At T4, a distinct inshore–off-

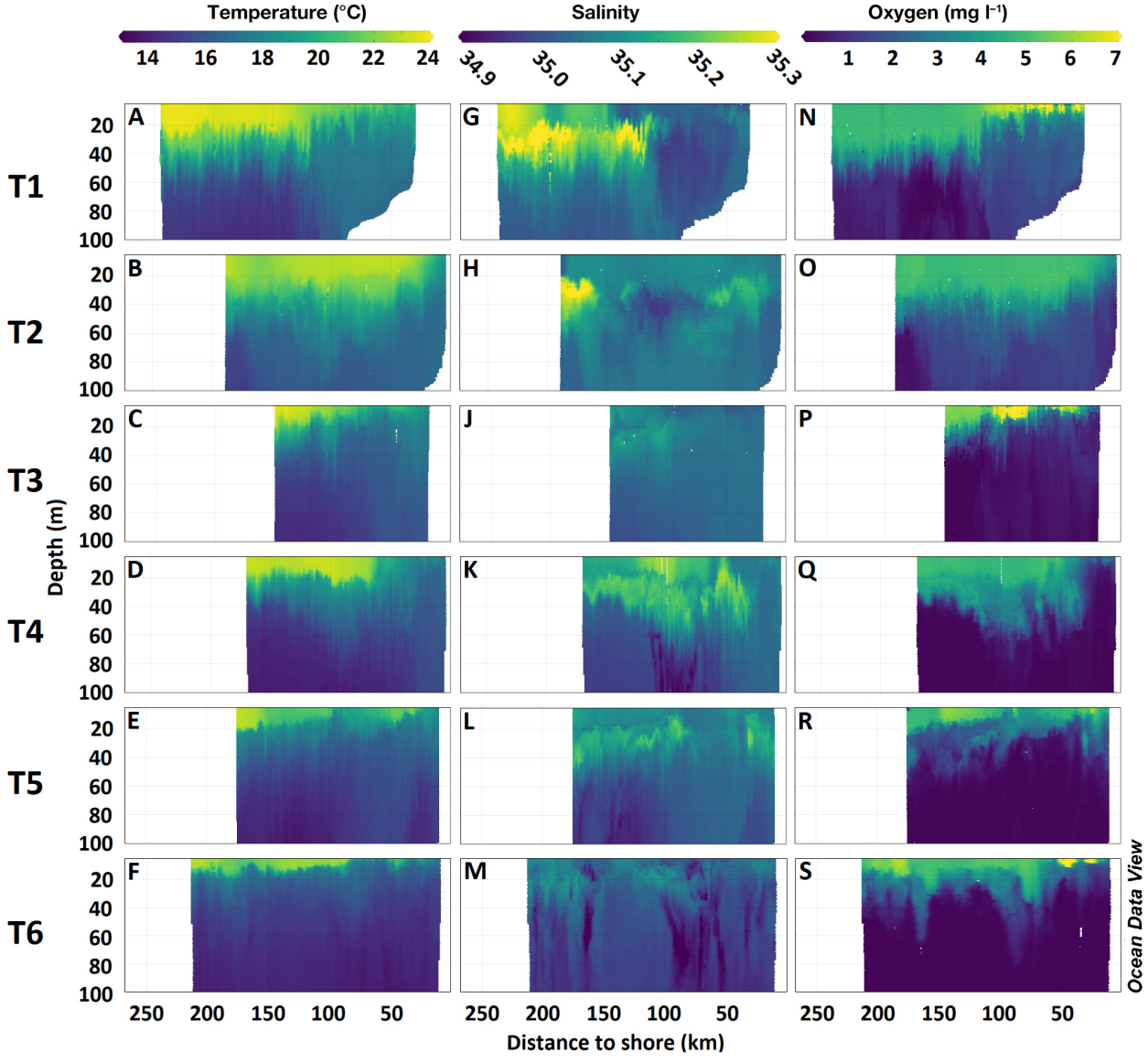

Fig. 3. ScanFish transect profiles of (A–F) temperature, (G–M) salinity and (N–S) dissolved oxygen concentration along each of the 6 transects (T1–T6) in the Humboldt Upwelling System

shore shift from well mixed to stratified waters occurred at ~75 km distance to shore, whereas T3, T5 and T6 revealed a more diffuse inshore–offshore pattern with a tendency towards more homogenized water closer to the coast. The salinity data of the ScanFish CTD indicated subsurface maxima across all transects (Fig. 3G–M), although these maxima were more distinct at transects with moderate to stronger Ekman transport. At T1, a low saline water mass on the upper shelf (<100 km to shore) with less saline water than further offshore at that transect indicated potential lateral intrusion of recently upwelled water (Fig. 3G). Transects with low coastal upwelling, especially T3, revealed strong vertical homogeneity in salinity. At T5, an eddy structure was indicated by high vertical homogeneity interrupting the subsurface maximum of surrounding waters, and a stronger oxycline was observed in the southern sampling region (Fig. 3L). The vertical oxygen profile at all transects was characterized by an oxygen minimum zone extending from 20 to 60 m (upper edge) down to several hundred meters (Fig. 3N–S). At T1, the oxygen profile abruptly changed from waters >100 km to shore to water masses on the upper shelf (Fig. 3N). At stations progressively further from shore, the oxygenated layer reached deeper depths (dissolved oxygen: ~5 mg l^{-1} at mid-transect to further offshore). At stations <100 km to shore, the upper oxygenated water mass was much narrower (~7 mg l^{-1}). Oxygen concentrations below the oxycline tended to be higher inshore than offshore. At the other transects, no such prominent inshore–offshore pattern occurred. More remarkable was the general trend of shoaling of the upper oxygenated water layer and a tendency of decreasing oxygenation (to almost anoxic water) within the oxygen minimum zone towards the central and southern sampling area.

3.3. Mucous-mesh grazer community

The mucous-mesh grazer community was dominated by appendicularians (up to 255 ind. m^{-3}, mostly *Oikopleura longicauda*) and doliolids (up to 171 ind. m^{-3}, mostly *Doliolum nationalis*; Fig. 4). Salps occurred relatively infrequently at stations but their abundance was occasionally high (up to 195 ind. m^{-3}, mostly *Iasis cylindrica*). Small pyrosomes (up to

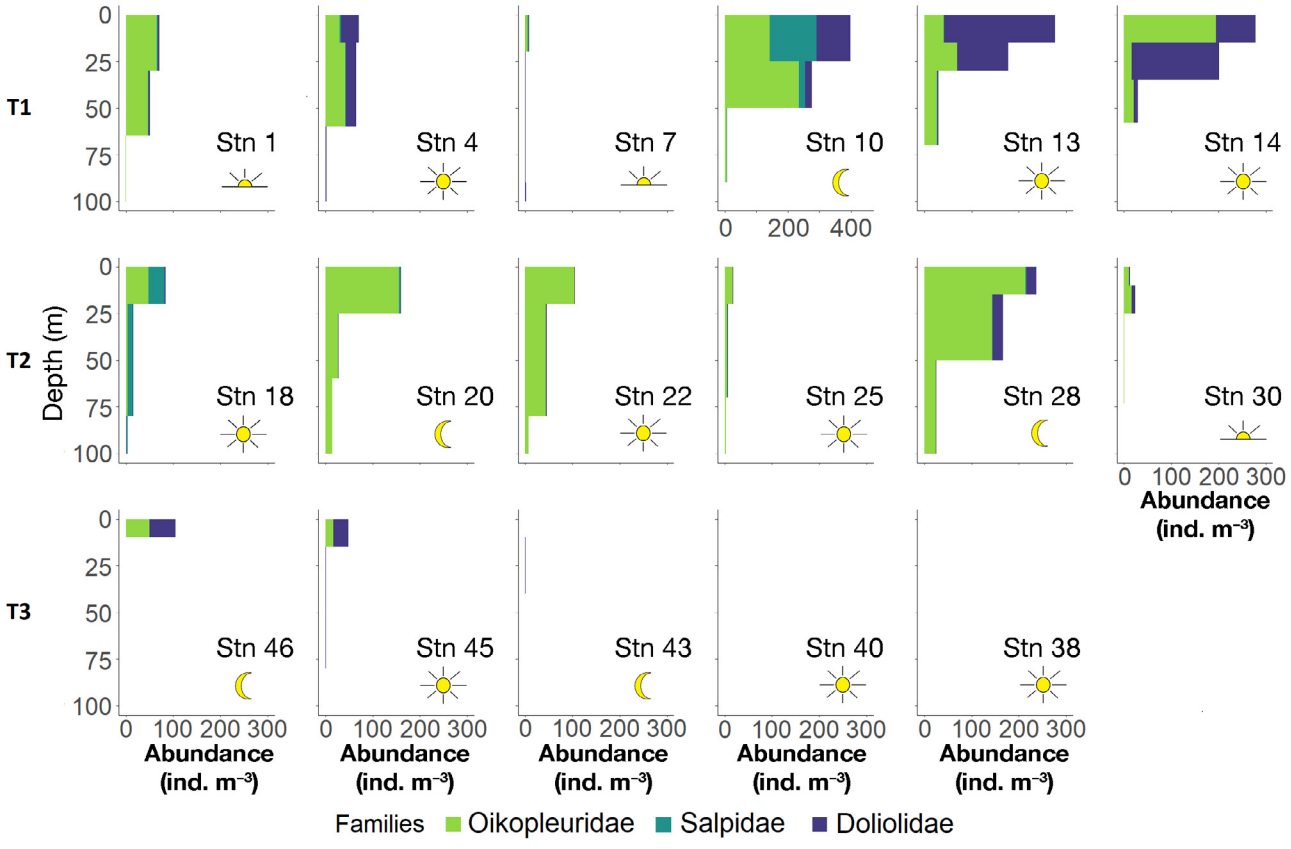

Fig. 4. Abundance of the more frequently encountered species of mucous-mesh grazers per station (Stn) and sampling depth at transects T1–T3. Note the different abundance scale at Stn 10. Sun and moon symbols indicate the time of day of sampling

2.4 ind. m^{-3}, only *Pyrosoma atlanticum*) as well as the gastropod families Cavolinidae (up to 3.7 ind. m^{-3}), Desmopteridae (up to 1.6 ind. m^{-3}) and Limacinidae (up to 8.0 ind. m^{-3}) were less abundant and fairly restricted to the northern sampling region. These numbers refer to the highest abundance per net. When integrating all 3 nets covering, in most cases, the upper 100 m, the maxima (ind. m^{-3}) were lower (appendicularians: 107, doliolids: 89, salps: 47, pyrosomes: 1.2, Cavolinidae: 1.2, Desmopteridae: 0.6, Limacinidae: 4.6).

At T1, abundance was distinctly higher at stations on the upper shelf (Stns 10–14) compared to further offshore (Stns 1–4, Fig. 4). At Stn 7, overlapping with the transition from largely well mixed to stratified water masses, the abundance was low compared to stations further inshore and offshore. A high abundance of salps was only found at Stn 10, whereas the remaining stations of T1 were dominated by either appendicularians or doliolids. At T2, the mucous-mesh grazer community was largely dominated by appendicularians that were highly variable in abundance. At T3, mucous-mesh grazer taxa were absent or occurred at very low abundance at the most coastal stations (Stns 43, 40 and 38). With increasing distance to shore, the abundance of doliolids and appendicularians increased. A similar pattern was found for T4, with a very high abundance of salps at Stn 53 (Fig. 5). At T5, doliolids were abundant at the coastal stations, whereas appendicularians were more abundant at Stns 78 and 80. At T6, mucous-mesh grazers only occurred in large numbers at the most offshore station, and salps were present at 2 of the 4 stations.

The rare taxa (Desmopteridae, Cavoliniidae, Limacinidae and Pyrosomatidae; Fig. 6) were largely restricted to T1 and T2. Except for the occurrence of Limacinidae and Cavoliniidae at low abundance at few stations (40, 80, 83 and 102), and slightly higher abundance of the same taxa at Stns 43, 45 and 99, there were no individuals present at the other stations along T3, T4, T5 and T6. Thus, these transects were excluded from graphs.

The vertical distribution was variable across taxonomic groups. In general, the abundance of mucous-mesh grazers was very low below the thermocline. Gastropods in the families Limacinidae and Desmopteridae (Fig. 6) were more abundant in the surface layers during nighttime compared to daytime hauls, and the WMD of Limacinidae was statistically signif-

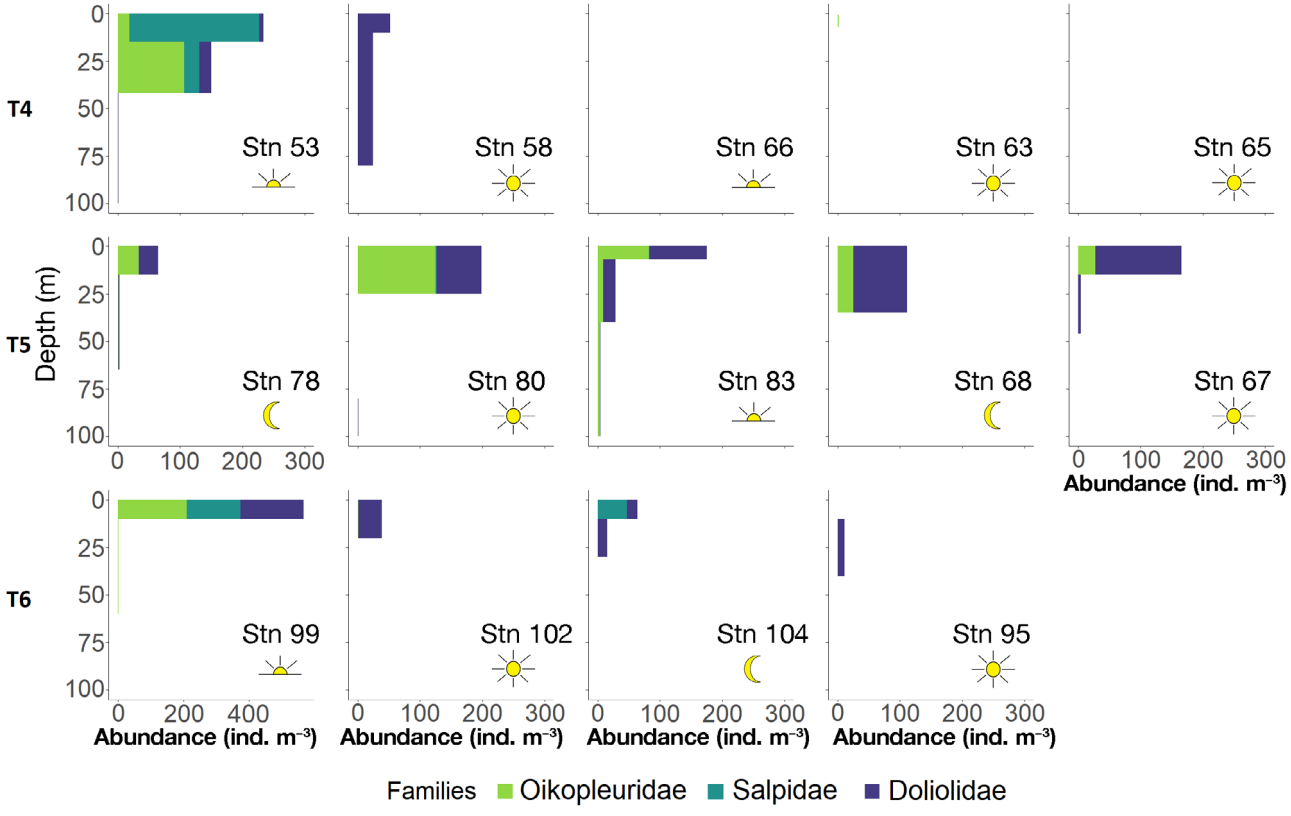

Fig. 5. Abundance of the more frequent species of mucous-mesh grazers per station (Stn) and sampling depth at transects T4–T6. Note the different abundance scale at Stn 99. Symbols as in Fig. 4

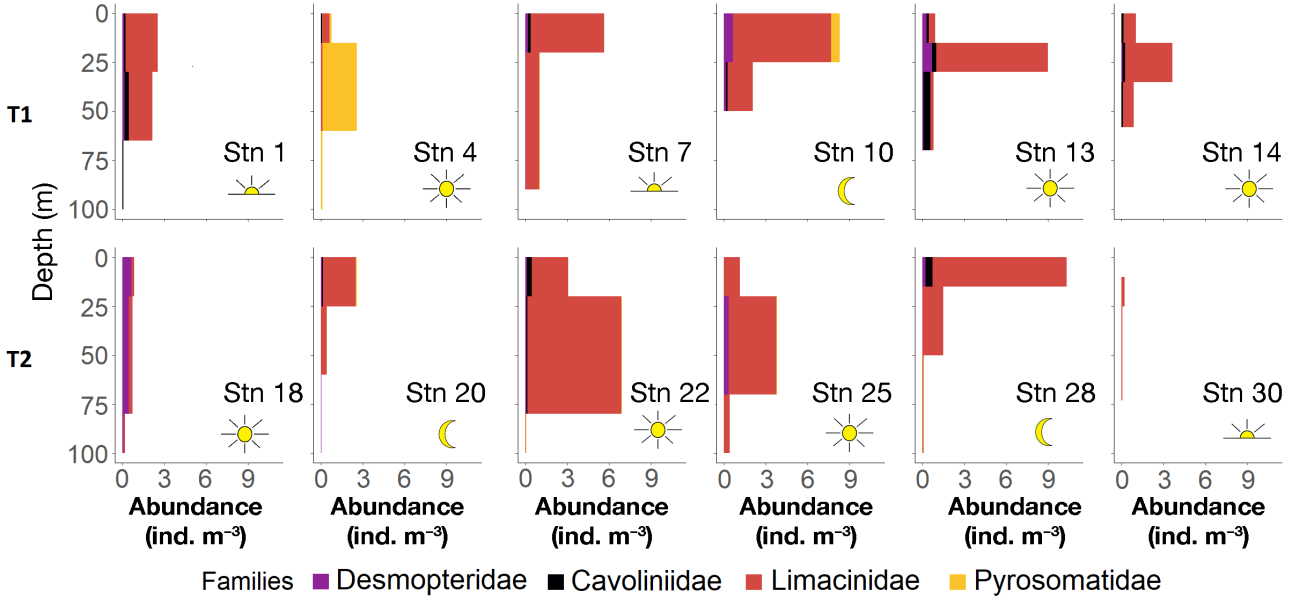

Fig. 6. Abundance of rare species per station (Stn) and sampling depth at transects T1 and T2. Symbols as in Fig. 4

icant between night and day ($p < 0.05$, $n = 21$). For tunicates, no diel differences in depth distribution were identified.

3.4. Abiotic drivers

Latitudinal differences were detected in the composition of the gelatinous zooplankton community (according to NMDS, Fig. 7). Especially the mucous-mesh grazer communities at stations northwards of T3 were more similar to each other in comparison to stations further south. Topographical categories, in contrast, did not appear to structure the community composition of mucous-mesh grazers in a consistent way. For 2-dimensional ordination, most factors appeared to be relevant ('ENVFIT' function), except for Ekman pumping during and prior to the sampling period, as well as salinity at all 3 depth intervals and turbidity at 31–50 and 51–70 m.

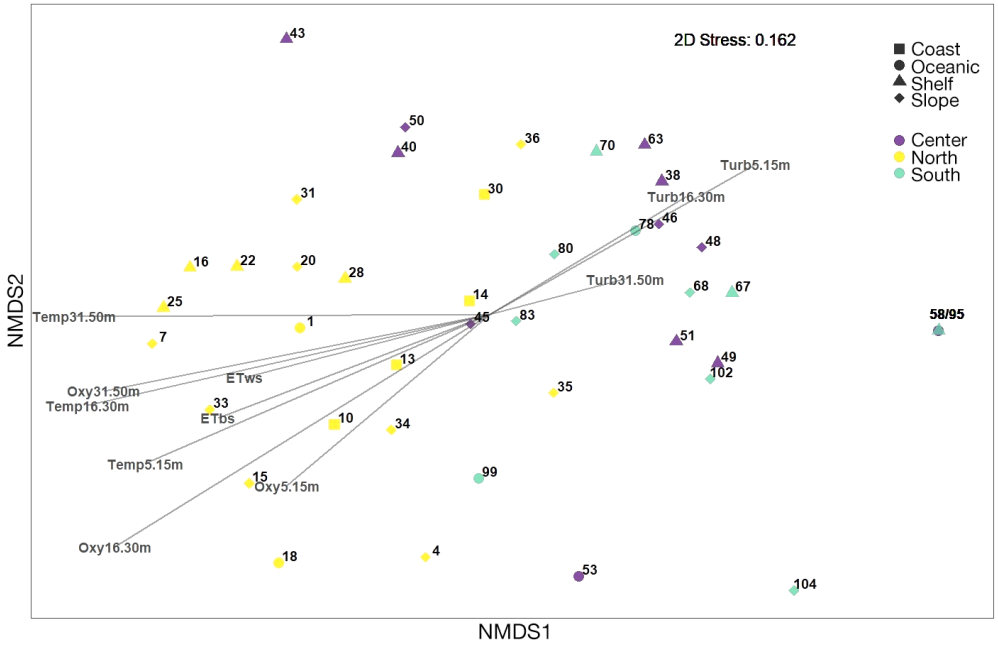

Fig. 7. Nonmetric multidimensional scaling (NMDS) of the mucous-mesh grazer community. Symbols are used to distinguish between latitudinal and inshore–offshore categories. To improve readability, not all variables and depth intervals are displayed. Hence, salinity and Ekman pumping, which were found to be of no relevance to the gelatinous species composition, were removed from the NMDS plot. Temp: temperature; Oxy: oxygen; Turb: turbidity; ET: Ekman transport; ws: 2 wk period of sampling; bs: 2 wk period before ws. Numbers such as '5.15m' describe the depth interval, in this case 5–15 m

3.5. Mucous-mesh grazers vs. chl *a* concentration vs. copepod abundance

In general, the maximum abundance of specific herbivorous/omnivorous copepods (dominated by *Calanus chilensis* and *Centropages hamatus*) was higher than that of mucous- mesh grazers across most of the sampling area (Fig. S2). However, the abundance of mucous-mesh grazers exceeded that of copepods at stations in northern coastal water masses (T1) and at offshore stations along T4 and T6. In contrast, herbivorous/omnivorous copepods were more widespread across the sampling area and most abundant at T3. Chl *a* concentrations were generally higher at stations that were relatively close (within 50 km) to shore. At coastal stations along T1 and T5, high chl *a* concentrations tended to be associated with a high abundance of mucous-mesh grazers, while at all other transects, increased mucous-mesh grazer abundance coincided with relatively low concentrations of chl *a*.

3.6. Grazing effect

The relative contribution of grazing in dominant copepods vs. gelatinous taxa was variable across transects and stations (Fig. 8). At T1 and T5, the ingestion rates of gelatinous species exceeded those of dominant copepod species at the most coastal stations. At T2, T4 and T6, however, the estimated ingestion rate of mucous-mesh grazer species was higher than that of copepod species at the offshore stations. At T3, the overall ingestion rate was estimated to be very high. The very high ingestion rate was almost exclusively related to high abundance of copepod species.

4. DISCUSSION

4.1. Species composition

The mucous-mesh grazer community within the HUS is largely understudied (Ayón et al. 2008). For a large fraction of gelatinous zooplankton species, including thaliaceans, the only data source from Peruvian waters is an unpublished, qualitative report from the Instituto del Mar del Perú (IMARPE). Regarding the species composition in the present study, the genera found are mostly included in the species list of Ayón et al. (2008). However, one remarkable new finding is the occurrence of pyrosomes (*Pyrosoma atlanticum*), which have not been previously described in Peruvian waters.

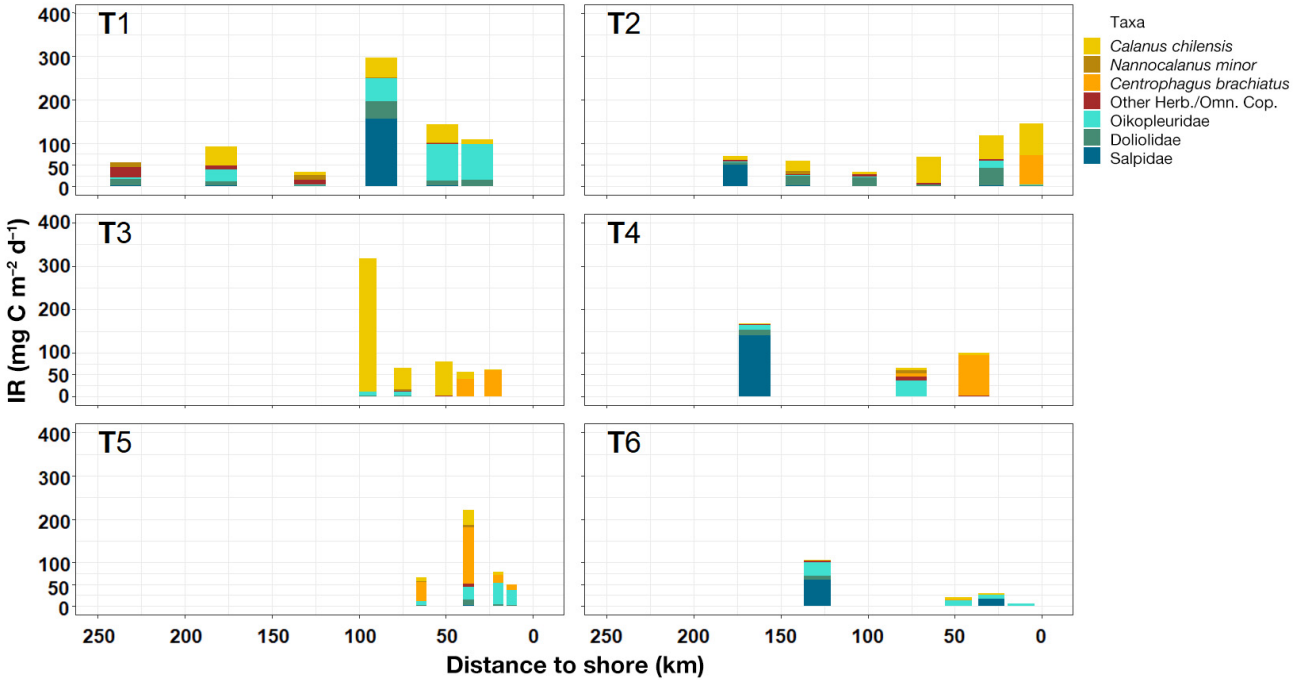

Fig. 8. Ingestion rate (IR) of dominant copepod species and mucous-mesh grazer families per transect (T1–T6) in the Humboldt Upwelling System

4.2. Vertical distribution

The HUS is well known for its sub-surface oxygen minimum zone (OMZ) constraining the depth distribution of most species sensitive to hypoxia to the upper ~20 to 50 m (Valdés et al. 2021). The OMZ influences the zooplankton community composition, vertical migration behavior and the resulting vertical carbon flux (Criales-Hernández et al. 2008, Kiko & Hauss 2019, Schukat et al. 2021). Although we suspect that a shallow thermocline/oxycline constrained diel vertical migration (DVM) behavior of most mucous-mesh feeders within the HUS, studies conducted on other systems with OMZs denoted species-specific differences in DVM, including vertical migration into waters with low oxygen concentrations (Maas et al. 2012). In the present study, the vertical distribution of mucous-mesh grazers such as appendicularians (e.g. *Oikopleura longicauda*) was largely restricted to oxygenated water masses above and within the thermocline.

Small-scale DVM, however, was suggested for several gastropod taxa in the present study migrating into the thermocline at daytime. Similarly, gastropods within the family Limacinidae were reported to conduct DVM within the Benguela Upwelling System (Koppelmann et al. 2013). Assessing patterns in DVM of highly mobile species such as pyrosomes is difficult since this group occurred at only a few stations and our sampling was confined to the upper 100 m of the water column while, for example, *P. atlanticum* has been reported to conduct DVM over several hundreds of meters (Andersen & Sardou 1994). The vertical distribution of salps has been reported to be diffuse during the daytime, with accumulation in surface waters during nighttime (Nogueira Júnior et al. 2015). This pattern would be challenging to detect in the present study given the infrequent occurrence of salps. The lack of doliolids in water masses below the thermocline is not surprising since this group has been reported to avoid oxygen-deficient water masses in the Canary Current system (Hoving et al. 2020). All in all, oxygen potentially plays an important role in the vertical structuring of mucous-mesh grazers, especially in the south (e.g. between 14 and 16°S), where a thin (~20 m) layer of well-oxygenated surface water sits on top of a several hundred-meter deep OMZ. Our strategy of defining sampling depth bins (ranges) based on hydrographic conditions facilitated ecological comparisons within and among our 6 cross-shelf transects but made it difficult to resolve and compare patterns of diel vertical migration.

4.3. Spatial distribution of mucous-mesh grazers in the HUS

Thaliacean species have been reported to occur mainly in open-ocean waters, and only few species have been reported to be abundant in shelf waters (Deibel & Paffenhöfer 2009, Conley et al. 2018). In the present study, thaliaceans were most abundant in coastal waters, although mucous-mesh grazers were also highly abundant in surface waters at a few offshore stations along T4 and T6. Although pyrosomes had not previously been reported in Peruvian waters and only reported once in Chilean waters (Palma & Apablaza 2004), they were found at several stations in the northern region of the Peruvian shelf. Considering the sampling gear, the abundance of larger individuals might even be underestimated. This common, tropical tunicate has gained considerable research interest due to its mass occurrence between 2016 and 2018 within the Californian Current System, especially off Oregon, and its expansion to higher latitudes (Sutherland et al. 2018, Miller et al. 2019, Schram et al. 2020).

Similar to *P. atlanticum*, pelagic gastropod species were largely restricted to the northern Peruvian shelf, but their abundance was relatively low in comparison to pelagic tunicates. This restricted (low latitude) distribution of pelagic gastropods is not surprising, as the group was dominated (62% abundance) by the tropical/subtropical species *Limacina trochiformis*. Other abundant species such as *L. bulimoides* and *Desmopterus papilio* are also common in the Benguela Upwelling System (Dadon & Masello 1999, Koppelmann et al. 2013). Quesquén Liza (2005) also reported a clear decline in *L. trochiformis* from the northern to the central and southern Peruvian waters but also indicated that most gastropod species were equally distributed across latitudes, which does not agree with our findings. Since the data set in the present study are based only on a single cruise, we cannot derive clear conclusions from these differences.

In general, there is an extraordinarily high temporal and spatial variability in the reported distribution and abundance of gelatinous species. Thaliaceans often occur in patches, mostly 2–3 km wide but occasionally also reaching >100 km in diameter (Paffenhöfer & Lee 1987, Deibel & Paffenhöfer 2009, Everett et al. 2011, Takahashi et al. 2015). On the southeastern shelf of the USA, Paffenhöfer & Lee (1987) reported 10 d increases in abundance of 25- and 5-fold for salps and doliolids, respectively. Depending on the timing and the sampling location, abundance varied by several orders of magnitude. For example,

Deibel & Paffenhöfer (2009) listed peak abundances of salps from 17 studies of 1.6 to >700 ind. m^{-3} and from 14 studies on doliolids ranging from 8 to 48 000 ind. m^{-3}. These fluctuations and variations reported in the literature suggest that, rather than comparing abundances across studies and systems, more information can be gained by comparing the potential abiotic and biotic drivers (or oceanographic structuring) of the mucous-mesh grazer community.

The abundance values for the smallest taxa (appendicularians, doliolids) could have been slightly underestimated, since a mesh size of 300 µm may not catch these sizes quantitatively. However, the large number of individuals indicated a high catch efficiency for these taxa.

4.4. Potential drivers of mucous-mesh grazer abundance

The NMDS analysis indicates high relevance of the drivers temperature, oxygen and turbidity. Due to the limitations previously described, this section will encompass a discussion on a more comprehensive set of potential drivers affecting the mucous-mesh grazer community. During the sampling period, the water masses off Peru were characterized by typical latitudinal patterns in Ekman transport and Ekman pumping. Peaks in coastal upwelling and Ekman transport occurred in the north and around 14° S, whereas Ekman pumping displayed the inverse pattern. Following known surface water mass characteristics based on temperature and salinity ranges (Ayón et al. 2008, Aronés et al. 2009), the upper water masses studied can largely be described as either 'subtropical surface water' or 'cold coastal water'. The mollusk and pyrosome distribution can be assumed to be mostly driven by the occurrence of warm water, due to the dominance of tropical to subtropical species. For example, *L. trochiformis*, the dominant gastropod species in this study, was restricted to water masses >16.8°C in the Atlantic and preferred temperatures >24°C (Chen & Bé 1964). Temperature might also be a main factor associated with the high abundance of *P. atlanticum* in the northern sampling area, since the occurrence of this species in the California Current was associated with marine heat waves in the previous years (Miller et al. 2019). Moreover, water temperature appears to be a key factor impacting the distribution of thaliaceans. Although the occurrence of salps has often been associated with colder water masses, the distribution of salps was too patchy in the present study to reveal any potential driver(s) of their spatial dynamics. On the other hand, the abundance of the dominant doliolids (*Doliolum* spp., mostly *D. nationalis* and *D. denticulatum*) has been associated with relatively warm-water masses in the Kuroshio (Lavaniegos & Ohman 2003, Ishak et al. 2020, 2022). Currents and warm temperatures appear to be the drivers of the distribution and abundance of these species in northern regions of the HUSs.

Even though doliolids were only found in northern (warm) waters, their peak abundance was in comparably cold, freshly upwelled water further inshore. Support for upwelling being the main driver of the formation of doliolid patches comes from the results of several studies conducted along the eastern US coast, where the formation of large thaliacean patches (mainly *Thalia democratica* and *Dolioletta gegenbauri*) was related to intrusions of nutrient-rich cold water (Paffenhöfer & Lee 1987, Deibel & Paffenhöfer 2009). Additional studies confirm the importance of upwelling for the distribution and abundance of thaliaceans (Paffenhöfer & Lee 1987, González et al. 2000, Li et al. 2011, Martin et al. 2017). In contrast, Lavaniegos & Ohman (2003) reported that upwelling did not affect the long-term abundance of tunicates in the California Upwelling System. Although Ekman transport was suggested to be less relevant than temperature, oxygen and turbidity in shaping the spatial distribution of tunicates in the present HUS study, the analysis (BIOENV) could be biased since only one Ekman transport value is provided per latitude, whereas CTD data were collected at each station.

The abundance of appendicularians was positively related to warm temperature and decreased pH in a Norwegian mesocosm study (Winder et al. 2017), but other studies have reported year-round production at varying temperatures (Tomita et al. 1999, Yebra et al. 2022) or the importance of phytoplankton production as a key driver. In Japanese waters, for example, the abundance of *Oikopleura longicauda* was related to chl *a*, rather than physical factors (Tomita et al. 2003). In the present study, the largely restricted vertical distribution to upper water masses was unrelated to spatial patterns of chl *a*. Appendicularian houses can get clogged more easily and discarded more often at high diatom abundance (Sato et al. 2001). Furthermore, not merely the quantity but also the size of prey particles is highly relevant for rates of filtering and ingestion by this group (Tiselius et al. 2003).

Analyzing the trophic interactions and potential effects of chl *a* concentration (bottom-up control) on the mucous-mesh grazers in the present study is challenging. Although chl *a* was considered to be a pri-

mary driver for 'blooms' of dense thaliacean patches in other areas (Deibel & Paffenhöfer 2009), there was little correspondence between chl *a* concentration and thaliacean abundance across HUS stations. Although there was some evidence for the bottom-up control of doliolids along T1 and T5, spatial co-occurrence of filter feeders and food is difficult to interpret; the strength of local grazing pressure and potential for top-down control on phytoplankton communities is not known. Furthermore, there was little overlap between patterns of distribution of mucous-mesh grazers and herbivorous/omnivorous copepods. A broader, trophodynamic view is needed (of a variety of predators and prey) as well as process studies (e.g. *in situ* incubations) to make robust statements on biotic drivers of spatial distribution. Furthermore, small-scale (local) features might be more relevant than large-scale dynamics within upwelling areas for structuring the plankton community (Bode et al. 2013, Bertrand et al. 2014). We highlight an example using continuous ScanFish CTD data and the correspondence between what appears to be laterally intruded upwelled water masses and higher mucous-mesh grazer abundance at T1. Thaliaceans, having one of the highest reported somatic growth rates of all multicellular animals, high rates of asexual reproduction and short generation times (Lucas & Dawson 2014), can rapidly form dense patches in response to favorable oceanographic conditions (Paffenhöfer & Lee 1987).

4.5. Ecological role of mucous-mesh grazers in the HUS

In general, the latitudinal differences in the abundance of mucous-mesh grazers along the Peruvian shelf area implied large differences in the ecological importance of these animals in the north versus the south of the HUS during our sampling campaign. Their higher abundance than dominant copepods combined with estimated rates of ingestion in the northern sampling region and at offshore stations on T4 and T6 suggests that mucous-mesh grazers can, at least temporally, play an important trophodynamic role within the zooplankton community off Peru. Nonetheless, it must be clearly stated that our results only provide a rough estimate of grazing effects, since first, ingestion rates of single species were assigned to the broader taxonomical family level, and second, size-related differences of ingestion rates were not taken into account. Furthermore, the data represent a snapshot of a dynamic system. Lavaniegos & Ohman (2003) described the long-term dynamics of cold and warm phases in the California Current and corresponding population dynamics of various tunicates, providing a classification of tunicates into cold-water and more persistent communities. Such classifications cannot be provided within our study. Nonetheless, we suggest that the spatial upwelling patterns, which correspond to the climatological pattern within this time of year, potentially favor repeated high abundance of mucous-mesh grazers. Bertrand et al. (2014) showed that spatial dynamics of seascape are mostly driven by ocean dynamics at scales less than 10 km. The high variability in abundance, especially the large accumulation of mucous-mesh grazers in freshly upwelled water along T1 strengthens the outcomes of Bertrand et al. (2014). A better understanding of spatiotemporal dynamics will require further sampling periods.

Assessing the trophodynamic role of mucous-mesh grazers in the HUS and elsewhere is hampered by large uncertainties in estimates of their clearance and ingestion rates. For example, the range in clearance rates reported for the salp *Pegea confoederata* exceeded one order of magnitude depending on the method applied (Sutherland & Thompson 2022). For the doliolid *D. denticulatum*, Katechakis et al. (2004) reported ingestion rates from 0.01 to 68.0 µg C ind.$^{-1}$ d^{-1}, while Alldredge (1977) reported water clearance rates of different appendicularian species that ranged from 36 to 1400 ml ind.$^{-1}$ h^{-1}. Furthermore, rates measured in the laboratory by pigment measurements, defecation rates and particle depletion can underestimate *in situ* rates (Sutherland & Madin 2010). Despite these uncertainties, ingestion and clearance rates of mucous-mesh grazers generally exceed those of crustacean species (Katechakis et al. 2004, Conley et al. 2018). González et al. (2000) indicated that the grazing rate of one salp species (*Salpa fusiformis*) formed almost 50% of the grazing rate of the entire crustacean zooplankton community in Chilean waters. Therefore, given the relative abundances and estimated ingestion rates of these consumers, it is not unreasonable to assume that a large flux of lower trophic level carbon is shunted to tunicates in newly upwelled waters in the north and at offshore stations in the south of our HUS sampling area. The implications of the high abundance of members of the mucous-mesh community in coastal waters known to be a spawning ground for Peruvian anchovy are unclear but potentially very important to study using not only broad-scale monitoring (this study) but also small-scale process investigations.

Acknowledgements. This study is embedded in the BMBF-funded project CUSCO – Coastal Upwelling System in a Changing Ocean. We thank the captain and crew of the RV 'Maria S. Merian' for their great work and help during the cruise. Furthermore, we thank Dr. Holger Auel for being the scientific leader during the cruise. We thank Dr. Bettina Martin and Silke Janssen from University Hamburg for their tireless effort during the preparation and sampling phase of cruise MSM80. Additionally, we thank all cruise participants for their collaborative work. A special thanks goes to Elda Luz Pinedo Arteaga and Jonathan Angello Correa Acosta, our IMARPE colleagues, for sharing their taxonomical knowledge and to the team of the University of Bremen for sharing laboratory equipment whenever needed.

LITERATURE CITED

Alldredge AL (1977) House morphology and mechanisms of feeding in the Oikopleuridae (Tunicata, Appendicularia). J Zool 181:175–188

Amante C, Eakins BW (2009) ETOPO1 arc-minute global relief model: procedures, data sources and analysis. NOAA Tech Memo NESDIS NGDC-24

Andersen V, Sardou J (1994) *Pyrosoma atlanticum* (Tunicata, Thaliacea): diel migration and vertical distribution as a function of colony size. J Plankton Res 16:337–349

Aronés K, Ayón P, Hirche HJ, Schwamborn R (2009) Hydrographic structure and zooplankton abundance and diversity off Paita, northern Peru (1994 to 2004) — ENSO effects, trends and changes. J Mar Syst 78:582–598

Ayón P, Criales-Hernandez MI, Schwamborn R, Hirche HJ (2008) Zooplankton research off Peru: a review. Prog Oceanogr 79:238–255

Bakun A, Weeks SJ (2008) The marine ecosystem off Peru: What are the secrets of its fishery productivity and what might its future hold? Prog Oceanogr 79:290–299

Bertrand A, Grados D, Colas F, Bertrand S and others (2014) Broad impacts of fine-scale dynamics on seascape structure from zooplankton to seabirds. Nat Commun 5:5239

Bode A, Álvarez-Ossorio MT, Miranda A, Ruiz-Villarreal M (2013) Shifts between gelatinous and crustacean plankton in a coastal upwelling region. ICES J Mar Sci 70:934–942

Boero F, Bouillon J, Gravili C, Miglietta MP, Parsons T, Piraino S (2008) Gelatinous plankton: irregularities rule the world (sometimes). Mar Ecol Prog Ser 356:299–310

Brochier T, Lett C, Fréon P (2011) Investigating the 'northern Humboldt paradox' from model comparisons of small pelagic fish reproductive strategies in eastern boundary upwelling ecosystems. Fish Fish 12:94–109

Boyd CM, Smith SL, Cowles TJ (1980) Grazing patterns of copepods in the upwelling system off Peru. Limnol Oceanogr 25:583–596

Chavez FP, Messié M (2009) A comparison of Eastern Boundary Upwelling ecosystems. Prog Oceanogr 83:80–96

Chavez FP, Bertrand A, Guevara-Carrasco R, Soler P, Csirke J (2008) The northern Humboldt Current System: brief history, present status and a view towards the future. Prog Oceanogr 79:95–105

Chen C, Bé AWH (1964) Seasonal distributions of euthecosomatous pteropods in the surface waters of five stations in the western North Atlantic. Bull Mar Sci Gulf Caribb 14: 185–220

Cole J, McGlade J (1998) Clupeoid population variability, the environment and satellite imagery in coastal upwelling systems. Rev Fish Biol Fish 8:445–471

Conley KR, Lombard F, Sutherland KR (2018) Mammoth grazers on the ocean's minuteness: a review of selective feeding using mucous meshes. Proc R Soc B 285:20180056

Criales-Hernández MI, Schwamborn R, Graco M, Ayón P, Hirche HJ, Wolff M (2008) Zooplankton vertical distribution and migration off Central Peru in relation to the oxygen minimum layer. Helgol Mar Res 62:85–100

Cuevas LA, Daneri G, Jacob B, Montero P (2004) Microbial abundance and activity in the seasonal upwelling area off Concepción (~36° S), central Chile: a comparison of upwelling and non-upwelling conditions. Deep Sea Res II 51:2427–2440

Dadon JR, Masello JF (1999) Mechanisms generating and maintaining the admixture of zooplanktonic molluscs (Euthecosomata: Opistobranchiata: Gastropoda) in the Subtropical Front of the South Atlantic. Mar Biol 135: 171–179

Deibel D, Lowen B (2012) A review of the life cycles and life-history adaptations of pelagic tunicates to environmental conditions. ICES J Mar Sci 69:358–369

Deibel D, Paffenhöfer GA (2009) Predictability of patches of neritic salps and doliolids (Tunicata, Thaliacea). J Plankton Res 31:1571–1579

Espinoza P, Bertrand A (2008) Revisiting Peruvian anchovy (*Engraulis ringens*) trophodynamics provides a new vision of the Humboldt Current system. Prog Oceanogr 79:215–227

Everett JD, Baird ME, Suthers IM (2011) Three-dimensional structure of a swarm of the salp *Thalia democratica* within a cold-core eddy off southeast Australia. J Geophys Res Oceans 116:C12046

FAO (2021) FAO Yearbook. Fishery and aquaculture statistics 2019. Food and Agriculture Organization (FAO), Rome. https://www.fao.org/fishery/en/publication/287024

González HE, Sobarzo M, Figueroa D, Nöthig EM (2000) Composition, biomass and potential grazing impact of the crustacean and pelagic tunicates in the northern Humboldt Current area off Chile: differences between El Niño and non-El Niño years. Mar Ecol Prog Ser 195:201–220

González HE, Giesecke R, Vargas CA, Pavez M and others (2004) Carbon cycling through the pelagic foodweb in the northern Humboldt Current off Chile (23° S). ICES J Mar Sci 61:572–584

Gruber N, Lachkar Z, Frenzel H, Marchesiello P and others (2011) Eddy-induced reduction of biological production in eastern boundary upwelling systems. Nat Geosci 4: 787–792

Hansen B, Bjørnsen PK, Hansen PJ (1994) The size ratio between planktonic predators and their prey. Limnol Oceanogr 39:395–403

Henschke N, Everett JD, Richardson AJ, Suthers IM (2016) Rethinking the role of salps in the ocean. Trends Ecol Evol 31:720–733

Hoving HJT, Neitzel P, Hauss H, Christiansen S and others (2020) In situ observations show vertical community structure of pelagic fauna in the eastern tropical North Atlantic off Cape Verde. Sci Rep 10:21798

Ishak NHA, Tadokoro K, Okazaki Y, Kakehi S, Suyama S, Takahashi K (2020) Distribution, biomass, and species composition of salps and doliolids in the Oyashio–Kuroshio transitional region: potential impact of massive bloom on the pelagic food web. J Oceanogr 76:351–363

Ishak NHA, Motoki K, Miyamoto H, Fuji T and others (2022) Basin-scale distribution of salps and doliolids in the tran-

sition region of the North Pacific Ocean in summer: drivers of bloom occurrence and effect on the pelagic ecosystem. Prog Oceanogr 204:102793

Katechakis A, Stibor H, Sommer U, Hansen T (2004) Feeding selectivities and food niche separation of *Acartia clausi, Penilia avirostris* (Crustacea) and *Doliolum denticulatum* (Thaliacea) in Blanes Bay (Catalan Sea, NW Mediterranean). J Plankton Res 26:589–603

Kiko R, Hauss H (2019) On the estimation of zooplankton-mediated active fluxes in oxygen minimum zone regions. Front Mar Sci 6:741

Koppelmann R, Kullmann B, Lahajnar N, Martin B, Mohrholz V (2013) Onshore–offshore distribution of Thecosomata (Gastropoda) in the Benguela Current upwelling region off Namibia: species diversity and trophic position. J Mar Biol Assoc UK 93:1625–1640

Lavaniegos BE, Ohman MD (2003) Long-term changes in pelagic tunicates of the California Current. Deep Sea Res II 50:2473–2498

Lawrence J, Töpper J, Petelenz-Kurdziel E, Bratbak G and others (2018) Viruses on the menu: the appendicularian *Oikopleura dioica* efficiently removes viruses from seawater. Limnol Oceanogr 63:S244–S253

Li K, Yin J, Huang L, Zhang J, Lian S, Liu C (2011) Distribution and abundance of thaliaceans in the northwest continental shelf of South China Sea, with response to environmental factors driven by monsoon. Cont Shelf Res 31: 979–989

Lucas CH, Dawson MN (2014) What are jellyfishes and thaliaceans and why do they bloom? In: Pitt K, Lucas C (eds) Jellyfish blooms. Springer, Dordrecht, p 9–44

Luo JY, Condon RH, Stock CA, Duarte CM, Lucas CH, Pitt KA, Cowen RK (2020) Gelatinous zooplankton-mediated carbon flows in the global oceans: a data-driven modeling study. Global Biogeochem Cycles 34:e2020GB006704

Luo JY, Stock CA, Henschke N, Dunne JP, O'Brien TD (2022) Global ecological and biogeochemical impacts of pelagic tunicates. Prog Oceanogr 205:102822

Maas AE, Wishner KF, Seibel BA (2012) The metabolic response of pteropods to acidification reflects natural CO_2-exposure in oxygen minimum zones. Biogeosciences 9: 747–757

Martin B, Koppelmann R, Kassatov P (2017) Ecological relevance of salps and doliolids in the northern Benguela Upwelling System. J Plankton Res 39:290–304

Miller RR, Santora JA, Auth TD, Sakuma KM, Wells BK, Field JC, Brodeur RD (2019) Distribution of pelagic thaliaceans, *Thetys vagina* and *Pyrosoma atlanticum*, during a period of mass occurrence within the California Current. CCOFI Rep 60:94–108

Neuer S, Cowles TJ (1994) Protist herbivory in the Oregon upwelling system. Mar Ecol Prog Ser 113:147–162

Nogueira Júnior M, Brandini FP, Codina JCU (2015) Diel vertical dynamics of gelatinous zooplankton (Cnidaria, Ctenophora and Thaliacea) in a subtropical stratified ecosystem (South Brazilian Bight). PLOS ONE 10:e0144161

Oksanen J, Blanchet FG, Friendly M, Kindt R and others (2020) vegan: community ecology package. https://cran.r-project.org/web/packages/vegan/vegan.pdf

Paffenhöfer GA, Lee TN (1987) Development and persistence of patches of Thaliacea. S Afr J Mar Sci 5:305–318

Palma S, Apablaza P (2004) Primer registro de *Pyrosoma atlanticum* Péron, 1804 en aguas costeras del Sistema de la Corriente de Humboldt (Tunicata, Thaliacea, Pyrosomatidae). First record of *Pyrosoma atlanticum* Péron, 1804 in the coastal waters of Humboldt System Current (Tunicata, Thaliacea, Pyrosomatidae). Invest Mar 32:133–136 (in Spanish with English abstract)

Pauly D, Christensen V (1995) Primary production required to sustain global fisheries. Nature 374:255–257

Pearre S Jr (1973) Vertical migration and feeding in *Sagitta elegans* Verrill. Ecology 54:300–314

Perissinotto R, Pakhomov EA (1998) Contribution of salps to carbon flux of marginal ice zone of the Lazarev Sea, Southern Ocean. Mar Biol 131:25–32

Quesquén Liza R (2005) Moluscos holoplanctónicos heteropoda y pteropoda colectados en noviembre y diciembre de 1996 en el mar peruano. BSc thesis, Ricardo Palma University, Lima

Rocke E, Cheung S, Gebe Z, Dames NR, Liu H, Moloney CL (2020) Marine microbial community composition during the upwelling season in the Southern Benguela. Front Mar Sci 7:255

Rossi V, López C, Hernández-García E, Sudre J, Garçon V, Morel Y (2009) Surface mixing and biological activity in the four Eastern Boundary Upwelling Systems. Nonlinear Process Geophys 16:557–568

Ryther JH (1969) Photosynthesis and fish production in the sea. Science 166:72–76

Sato R, Tanaka Y, Ishimaru T (2001) House production by *Oikopleura dioica* (Tunicata, Appendicularia) under laboratory conditions. J Plankton Res 23:415–423

Schram JB, Sorensen HL, Brodeur RD, Galloway AWE, Sutherland KR (2020) Abundance, distribution, and feeding ecology of *Pyrosoma atlanticum* in the Northern California Current. Mar Ecol Prog Ser 651:97–110

Schukat A, Teuber L, Hagen W, Wasmund N, Auel H (2013) Energetics and carbon budgets of dominant calanoid copepods in the northern Benguela upwelling system. J Exp Mar Biol Ecol 442:1–9

Schukat A, Hagen W, Dorschner S, Acosta JC, Arteaga ELP, Ayón P, Auel H (2021) Zooplankton ecological traits maximize the trophic transfer efficiency of the Humboldt current upwelling system. Prog Oceanogr 193:102551

Scura ED, Jerde CW (1977) Various species of phytoplankton as food for larval northern anchovy, *Engraulis mordax*, and relative nutritional value of the dinoflagellates *Gymnodinium splendens* and *Gonyaulax polyedra.* Fish Bull 75:577–583

Steedman HF (1976) Zooplankton fixation and preservation. Monographs on oceanographic methodology, Vol 4. Unesco Press, Paris

Sutherland KR, Madin LP (2010) A comparison of filtration rates among pelagic tunicates using kinematic measurements. Mar Biol 157:755–764

Sutherland KR, Thompson AW (2022) Pelagic tunicate grazing on marine microbes revealed by integrative approaches. Limnol Oceanogr 67:102–121

Sutherland KR, Sorensen HL, Blondheim ON, Brodeur RD, Galloway AWE (2018) Range expansion of tropical pyrosomes in the northeast Pacific Ocean. Ecology 99: 2397–2399

Takahashi K, Ichikawa T, Fukugama C, Yamane M and others (2015) In situ observations of a doliolid bloom in a warm water filament using a video plankton recorder: bloom development, fate, and effect on biogeochemical cycles and planktonic food webs. Limnol Oceanogr 60: 1763–1780

Taylor MH, Tam J, Blaskovic V, Espinoza P and others (2008) Trophic modeling of the Northern Humboldt Cur-

rent Ecosystem, Part II: elucidating ecosystem dynamics from 1995 to 2004 with a focus on the impact of ENSO. Prog Oceanogr 79:366–378

Tiselius P, Petersen J, Nielsen T, Maar M and others (2003) Functional response of *Oikopleura dioica* to house clogging due to exposure to algae of different sizes. Mar Biol 142:253–261

Tomita M, Ikeda T, Shiga N (1999) Production of *Oikopleura longicauda* (Tunicata: Appendicularia) in Toyama Bay, southern Japan Sea. J Plankton Res 21:2421–2430

Tomita M, Shiga N, Ikeda T (2003) Seasonal occurrence and vertical distribution of appendicularians in Toyama Bay, southern Japan Sea. J Plankton Res 25:579–589

Valdés J, Sifeddine A, Guiñez M, Castillo A (2021) Oxygen minimum zone variability during the last 700 years in a coastal upwelling area of the Humboldt system (Mejillones, 23° S, Chile). A new approach from geochemical signature. Prog Oceanogr 193:102520

Vargas CA, González HE (2004) Plankton community structure and carbon cycling in a coastal upwelling system. I. Bacteria, microprotozoans and phytoplankton in the diet of copepods and appendicularians. Aquat Microb Ecol 34:151–164

Vargas CA, Martínez RA, Cuevas LA, Pavez MA and others (2007) The relative importance of microbial and classical food webs in a highly productive coastal upwelling area. Limnol Oceanogr 52:1495–1510

Winder M, Bouquet JM, Bermúdez JR, Berger SA and others (2017) Increased appendicularian zooplankton alter carbon cycling under warmer more acidified ocean conditions. Limnol Oceanogr 62:1541–1551

Yebra L, Puerto M, Valcárcel-Pérez N, Putzeys S, Gómez-Jakobsen F, García-Gómez C, Mercado JM (2022) Spatio-temporal variability of the zooplankton community in the SW Mediterranean 1992–2020: linkages with environmental drivers. Prog Oceanogr 203:102782

Editorial responsibility: Deborah K. Steinberg, Gloucester Point, Virginia, USA
Reviewed by: N. Ishak and 2 anonymous referees

Submitted: November 24, 2022
Accepted: September 28, 2023
Proofs received from author(s): December 6, 2023